

# Photodissociative I<sup>127</sup> laser in a magnetic field

I. M. Belousova, B. D. Bobrov, V. M. Kiselev, V. N. Kurzenkov, and  
P. I. Krepostnov

(Submitted March 20, 1973)

Zh. Eksp. Teor. Fiz. 65, 524-536 (August 1973)

Results are presented of an investigation of the effect of a magnetic field and of a number of other factors on the kinetics of the emission spectrum of a photodissociative laser operating on the  $^2P_{1/2}$ - $^2P_{3/2}$  iodine atom transition.

## INTRODUCTION

Experimental data on the effect of a magnetic field on the operation of a laser are essential for the understanding of the generation mechanism because by influencing this mechanism it is possible to produce radiation with given parameters, e.g., given frequency, polarization, and output power. Some of the properties of the photodissociative laser in a magnetic field have already been described in the literature.<sup>[1,2]</sup> It is important to note at the outset that, in contrast to lasers using electrical discharges in gases, in the case of the photodissociative laser the Zeeman effect is observed under more favorable conditions because the magnetic field does not then affect the pumping process and the so-called optical plasma effects are absent.<sup>[3]</sup> The broadening of the amplification profile in the photodissociative laser is homogeneous in character and, therefore, the amplification of the stimulated emission in different parts of the profile is due to the same atoms (if we ignore their spatial distribution). Valleys on the amplified profile and the effects associated with them are absent. Because of the homogeneous broadening of the profile and the associated strong competition between the modes, only one longitudinal mode is generated by the photodissociative laser.

On the other hand, the photodissociative laser operates in magnetic fields  $50 < H < 15 \times 10^3$  Oe, and in such fields the interaction between the electronic (J) and nuclear (I) angular momenta of the iodine atoms with one another is comparable with their interaction with the external field.<sup>[5]</sup> The result is a nonlinear dependence of the frequencies of the Zeeman components on the field, and a continuous variation of the transition probabilities between the Zeeman sublevels as the field increases. There is no doubt that this substantially complicates any investigation of the behavior of the laser in a magnetic field. Moreover, because of the relatively rapid relaxation between the hyperfine structure sublevels of the  $^2P_{1/2}$  and  $^2P_{3/2}$  states, there is strong competition between the individual hyperfine splitting components,<sup>[1,2,6]</sup> which is particularly noticeable in the magnetic field which is always present under the working conditions of the laser.

In view of the above complications, the kinetics of the emission spectrum generated by a photodissociative laser in a magnetic field is not as yet fully understood, and new detailed studies of this process are essential. In this paper we consider some of the basic properties of the photodissociative laser in a magnetic field, and attempt to explain its behavior in terms of the results of an earlier theoretical analysis<sup>[5]</sup> of the Zeeman effect in the spontaneous emission through the working transition of the laser.<sup>[5]</sup>

## EXPERIMENTAL METHOD AND APPARATUS

In each working cycle we measured the following characteristics of the laser: the shape of the generated pulse, the polarization of the emitted radiation, the spectrum of the radiation, the shape of the pumping flash, the pressure of the working gas, and the external magnetic field. Three-channel spectrum detection was employed, so that with the use of Fabry-Perot etalons we could avoid the overlapping of the interference orders and, at the same time, measure with sufficient precision the separation of the generated spectral components. The apparatus is illustrated schematically in Fig. 1.

The working chamber, which had an internal diameter of 16 mm, was mounted between the poles of the electromagnet when a transverse magnetic field was employed, and along the axis of the solenoid when a longitudinal field was used. The ends of the chamber lay outside the electromagnet gap or the solenoid and were covered by a screen which was opaque to the pumping radiation. The length of the open part of the chamber was 300 mm. The length of the electromagnet poles was 360 mm and the width was 40 mm. The solenoid was 400 mm long. The electromagnet was supplied with direct current and produced a constant transverse magnetic field of up to 7 kOe. The maximum magnetic field produced by the solenoid was 1.6 kOe.

The working medium (C<sub>3</sub>F<sub>7</sub>I) was pumped by special coaxial lamps in which the current flowed in one direction along the discharge plasma and, in the return direction, along a metal rod mounted along the axis of the lamp. This ensured that the magnetic field on the surface of the lamp (diameter 35 mm) did not exceed 50 Oe. This field was reached only at the beginning of the pumping flash and fell to 10-20 Oe after 15-20 μsec. The magnetic field in the chamber (which lay at a distance of 100 mm from the lamps) did not exceed a few oersteds when the laser pulse was generated. The supplies for the lamps were also coaxial. To increase the light output of the pumping lamps we used reflectors made of aluminum foil. The maximum brightness temperature in the lamps was 13 000°K.

One of the laser mirrors had a constant reflection coefficient ( $r_1 = 99.5\%$ ) while the reflection coefficient of the exit mirror was varied ( $r_2 = 80, 40, \text{ and } 8\%$ ). In the spectrum recording system we used Fabry-Perot etalons with gaps of 3, 40, and 150 mm. The interference patterns produced by the etalons were recorded on film with the aid of electron-optical converters and the appropriate objective lenses. The interference patterns from the 3 and 150 mm etalons were time scanned, whilst the pattern from the 40 mm etalon was recorded statically. The resolution limit of the 3, 40, and 150

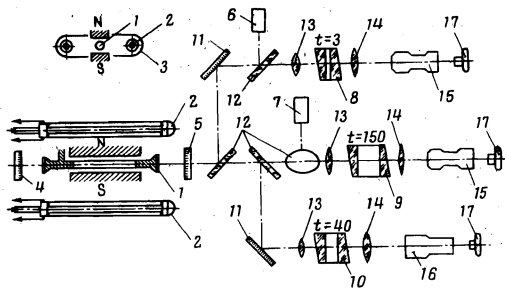


FIG. 1. Apparatus: 1—laser chamber; 2—pumping lamps; 3—reflector; 4, 5—resonator mirrors; 6, 7—photomultipliers; 8, 10—Fabry-Perot etalon; 11—rotated mirrors; 12—rotated plates; 13, 14—lenses and objectives; 15, 16—electron-optical converters; 17—cameras.

mm etalons was  $0.027$ ,  $0.002$ , and  $5.4 \times 10^{-4} \text{ cm}^{-1}$ , respectively. However, it was noted in<sup>[4]</sup> that the fundamental restriction on the resolution of the spectral channels was imposed by the properties of the electron-optical converters with the result that the maximum resolution achieved in practice was  $1.5 \times 10^{-3} \text{ cm}^{-1}$ .

The shape of the pumping flash was recorded with an FEU-18 photomultiplier, whilst the shape of the laser pulse was recorded simultaneously by two photomultipliers (FEU-28). The radiation was thrown onto the latter photomultipliers by rotated plates set at the Brewster angle to the laser axis in mutually perpendicular planes. These planes were oriented so that the photomultipliers recorded polarized radiation in which the electric vectors lay parallel and perpendicular to the magnetic field. This has enabled us to perform a qualitative study of the polarization of the laser radiation as a function of the magnetic field.

The constant magnetic field was measured by a standard Hall probe (F4354/1 magnetometer). The experimental uncertainty in the measured field was 2.5%.

## RESULTS

When there was no magnetic field, the spectrum of the stimulated radiation was substantially dependent on the pump energy. Thus, when the gas pressure was varied from 1 Torr up to 135 Torr, and a sufficiently strong pump intensity was employed (brightness temperature  $T_b = 10^4 \text{ K}$ ), the presence in the laser beam of components other than  $F = 3 - F = 4$  could not be detected. Very weak traces of a second component corresponding to the  $F = 2 - F = 2$  transition were recorded on the interference pattern only at the maximum possible pump energy under our conditions ( $T_b = 13\,000 \text{ K}$ ). These processes were observed at pressures between 20 and 90 Torr, since at lower pressures the necessary amplification probably could not be achieved for the 2—2 component. The 2—2 intensity was lower by about three orders of magnitude than the intensity of the 3—4 component. It is well known that the probability of the  $F = 2 - F = 2$  transition in zero magnetic fields is only slightly lower than the corresponding probability for the  $F = 3 - F = 4$  transition (in fact, by a factor of 2). A very high overall increase above the threshold is achieved for generation with  $T_b = 13\,000 \text{ K}$  (gain  $0.20 \text{ cm}^{-1}$ , losses  $0.02 \text{ cm}^{-1}$ ). Under these conditions the low intensity of the laser radiation corresponding to the 2—2 component, and its appearance near the threshold, can only be explained by strong competition between these components, which may occur as a result of the

sufficiently rapid relaxation of excited atoms between the  $F = 3$  and  $F = 2$  sublevels of the  $^2P_{1/2}$  state.<sup>[6]</sup>

The separation between the 3—4 and 2—2 components in zero magnetic field was found to be  $\Delta\nu = 0.460 \pm 0.003 \text{ cm}^{-1}$ . Using this value of  $\Delta\nu$  and the known separation between the  $F = 2$  and  $F = 4$  sublevels of the  $^2P_{3/2}$  state,<sup>[7]</sup> we can find the hyperfine structure constant for the  $^2P_{1/2}$  state. The result is  $A_{1/2} = 0.222 \pm 0.001 \text{ cm}^{-1}$ , which is in agreement with measurements on spontaneous emission.<sup>[8,9]</sup>

Figure 2a shows oscillograms of the laser pulse in zero magnetic field for mutually perpendicular polarizations. The intensities of the two signals are roughly the same, showing that the radiation is unpolarized. Figure 2b shows the oscillogram obtained in a transverse magnetic field of 100 Oe. As can be seen, there is a radical change. For the magnetic dipole transition which we are considering the  $\sigma$  component ( $\Delta m = 0$ ) corresponds to the upper signal, and the  $\pi$  component ( $\Delta m = \pm 1$ ) corresponds to the lower component. It follows that in a magnetic field of 100 Oe the polarization corresponding to the  $\sigma$  component is the predominant one. This relationship between the signal intensities remains in higher fields. In a field of 100 Oe, generation begins at the same time as in zero field, i.e., there is no appreciable change in the threshold. However, in a field of 200 Oe (Fig. 2c), generation appears somewhat later than in zero field, and in 300 Oe the delay is  $10 \mu\text{sec}$ , showing a clear rise of the threshold. Generation then occurs at a frequency corresponding to the  $F = 3 - F = 4$  transition and there is no emission due to the 2—2 transition. With a gas pressure of 22.5 Torr and  $T_b = 10^4 \text{ K}$ , the second component appears beginning with 350 Oe, and the intermediate situation obtains up to 440 Oe at which the intensity of the new component is found to predominate. Above 450 Oe the generation is confined to the second component (2—2 transition). For the moment, we classify the transition in accordance with the quantum number  $F$  since, as will be shown below, in fields of this order the Zeeman components of the original lines are not too far apart and each group of components forms a resultant profile. As before, the polarization of the radiation corresponds to the  $\sigma$  component. Figure 2d shows the generation pulse in a field of 500 Oe. As can be seen, the onset of generation is delayed relative to the onset in zero field.

Figure 3a illustrates the change in the emission spectrum for a working pressure of 22.5 Torr as the transverse magnetic field is increased. The pump corresponds to  $T_b = 10^4 \text{ K}$ . The first two components, 3—4 and 2—2, have already been discussed. All that remains is to note that the position of the 3—4 component remains the same to within  $3 \times 10^{-3} \text{ cm}^{-1}$  as the magnetic

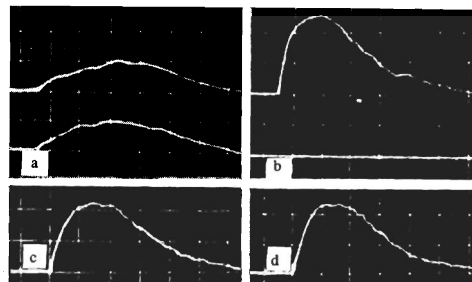


FIG. 2. Laser pulse oscillograms: a— $H = 0$ ; b— $H = 100 \text{ Oe}$ ; c— $H = 300 \text{ Oe}$ ; d— $H = 500 \text{ Oe}$ .

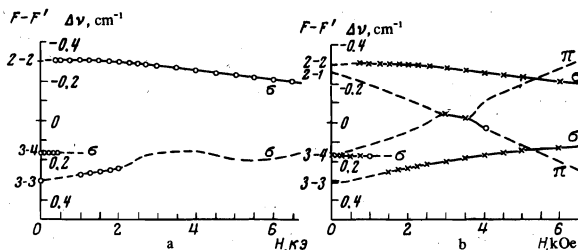


FIG. 3. Spectrum of stimulated radiation in a transverse magnetic field: a— $pC_3F_7I = 22.5$  Torr; b—points  $pC_3F_7I = 22.5$  Torr,  $p_{Ar} = 225$  Torr, crosses (and points coincident with them)— $pC_3F_7I = 22.5$  Torr,  $p_{Ar} = 375$  Torr.

field increases, until it disappears altogether. The 2—2 component shows an appreciable shift in fields in excess of 2000 Oe. Between 800 and 2000 Oe the generated radiation contains both the 2—2 component and a further component due to the  $F = 3 - F = 3$  transition. Its intensity at first increases, reaches a maximum between 1000 and 1500, and then falls again. In accordance with the behavior of the intensity of the 3—3 component, the delay of the onset of generation relative to the onset for  $H = 0$  decreases to practically zero at  $H = 1000$  Oe and then increases again, reaching about 12  $\mu\text{sec}$  in a field of 2000 Oe. Further increase in the field results in a reduction in this delay which is then equal to 6—8  $\mu\text{sec}$ . In fields between 2000 and 7000 Oe, only one spectral component corresponding to the 2—2 transition is generated.

The generation of the spectral components by the laser working in a magnetic field depends on the gas pressure in the chamber. Thus, other things being equal, for a working gas pressure of 3.75 Torr the 2—2 component appears in a field of 300 Oe, while at a pressure of 135 Torr it appears for a field of 600 Oe. When the total pressure is raised to 375 Torr by introducing argon as a buffer gas, the 2—2 component appears even for 900 Oe. There is also a change in the behavior of the other spectral components. Figure 3b shows the behavior of the spectrum of the stimulated radiation, as the magnetic field increases, for two gas pressures, namely, 247.5 and 397.5 Torr. Argon is used as the buffer gas. The pumping level again corresponds to  $T_b = 10^4$  K. The generated radiation contains a further spectral component whose position corresponds to the crossing of the shifted group of lines due to the 3—4 transition with the group of lines due to the 2—1 transition (see<sup>[5]</sup>). The appearance of this new component is accompanied by a change in the polarization of the laser beam. The intensity corresponding to the  $\sigma$  component is reduced, whilst that in the  $\pi$  component increases sharply.

When the longitudinal field is applied to the active medium, the signals from the two photomultipliers recording the different polarizations become equal in strength. This occurs because the polarization of the output radiation is now circular and corresponds to the group of  $\pi^*$  components of the  $F = 3 - F = 4$  transition (see<sup>[5]</sup>). The radiation frequency shifts continuously as the field strength increases. In a field of 800 Oe, the generated radiation contains a further component, the position of which shows that it corresponds to the group of  $\pi^-$  components of the  $F = 2 - F = 1$  transition. These components are present up to 1200 Oe. In higher fields the laser radiation contains only the lines corresponding to the group of  $\pi^-$  components of the  $F = 2 - F = 1$  transition. Figure 4 shows the spectral composition of

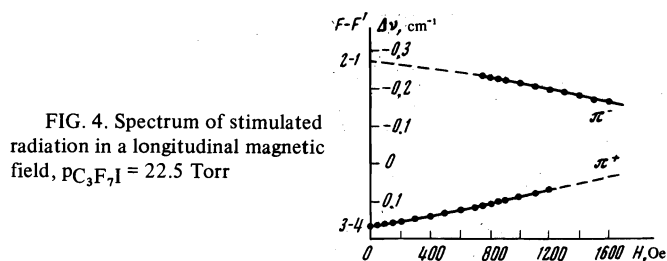


FIG. 4. Spectrum of stimulated radiation in a longitudinal magnetic field,  $pC_3F_7I = 22.5$  Torr

the laser radiation in a longitudinal magnetic field and working-gas pressure of 22.5 Torr. As the pressure increases, the  $F = 2 - F = 1$  components appear at still higher values of the magnetic field.

Let us now consider the time dependence of the components which are present simultaneously in the laser beam. Figure 5 shows the interference patterns recorded by time scanning when both the 2—2 and the 3—3 components were present. The field is transverse and varies between 1000 and 2000 Oe. The field strength determines the time of simultaneous generation of the components and their intensities. While in a field of 1000 Oe the intensities of the components and the generation times are comparable, in fields of 15 000 and 2000 Oe the 3—3 component is clearly weaker and the time for which it is present corresponds only to the maximum of the pumping flash. When the generation threshold in the magnetic field of 1000 Oe is increased by introducing losses (Fig. 5c), the competition between the components becomes much clearer. Correspondingly, by reducing the threshold or increasing the pumping level, we can obtain more stable generation in both components simultaneously even for a large difference between their gains. The same type of competition and instability is observed in other cases of simultaneous participation of components in generation.

When the magnetic field is not zero, there is a further type of instability which is illustrated by Fig. 5e. This figure shows the interference pattern for stimulated radiation obtained with the 150 mm Fabry-Perot etalon. The pattern clearly shows a wavelength instability, which is stronger in fields for which there are other components with similar gains, for field values near the

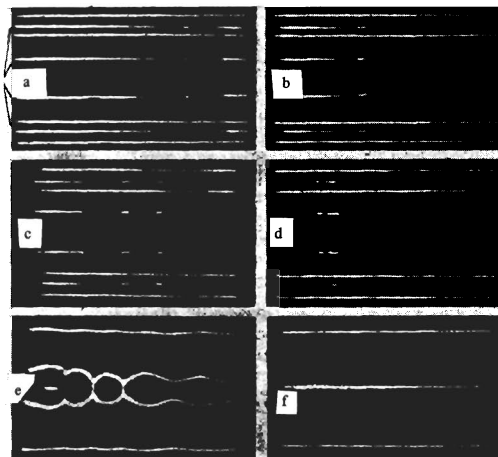


FIG. 5. Time-scanned interference pattern for the laser radiation ( $pC_3F_7I = 22.5$  Torr; pumping level corresponds to  $T_b = 10^4$  K, transverse magnetic field, scanning time 100  $\mu\text{sec}$ ); a— $H = 1000$  Oe; b—1500 Oe; c— $H = 1000$  Oe, losses introduced; d— $H = 2000$  Oe; e— $H = 500$  Oe; f— $H = 0$ . For cases a, b, c, and d the Fabry-Perot separation is 3 mm and in the remaining cases it is 150 mm.

times of switching. This instability appears to have the same origin as the previous one. The deviation varies in the range  $3 \times 10^{-3} - 4 \times 10^{-3} \text{ cm}^{-1}$ . The instantaneous line width is about  $0.0015 \text{ cm}^{-1}$  and there is moderate agreement with the value reported in<sup>[4]</sup>. For comparison, Figure 5e shows the pattern obtained with the 150 mm Fabry-Perot etalon in zero magnetic field. As can be seen, there is now no instability.

A change in the reflection coefficient of the exit mirror is found to affect, but to a lesser extent, the range of magnetic fields for which the simultaneous generation of different components is possible.

## ANALYSIS OF EXPERIMENTAL RESULTS

To explain some of the features of the spectrum of the stimulated radiation generated in a magnetic field, we shall use the theoretical analysis of the Zeeman effect for the iodine transition given in<sup>[5]</sup>, where for a broad range of magnetic fields calculations are reported of the probabilities of the strongest Zeeman components and of the complete frequency spectrum for the  $^2P_{1/2} - ^2P_{3/2}$  transition.

In the case of fast collisional relaxation over the Zeeman sublevels of the upper and lower states, all transitions which correspond to particular hyperfine structure components which are close in frequency (the separation between neighboring frequencies is not greater than the broadening of the individual transition) and have the same polarizations can be summed, and this yields the resultant gain curve for each polarization, which is determined by the probabilities of the individual Zeeman components. It can readily be shown that this resultant gain curve for transition between one of the sublevels of the  $^2P_{1/2}$  state with particular  $F$  and the  $^2P_{3/2}$  state which, because of the fast relaxation between its sublevels,<sup>[6]</sup> is considered to be degenerate and common to all the spectral components, can be written in the following form

$$k_{31}(\omega) = \frac{2\pi\omega\Delta\omega}{3\hbar c} \left[ \frac{n_2 + n_3}{g_2 + g_3} - \frac{n_1}{g_1} \right] \sum_{mm'} \frac{|(m|\hat{\mu}|m')|^2}{(\omega - \omega_0)^2 + (\Delta\omega)^2/4}, \quad (1)$$

$$k_{21}(\omega) = \frac{2\pi\omega\Delta\omega}{3\hbar c} \left[ \frac{n_2 + n_3}{g_2 + g_3} - \frac{n_1}{g_1} \right] \sum_{mm'} \frac{|(m|\hat{\mu}|m')|^2}{(\omega - \omega_0)^2 + (\Delta\omega)^2/4},$$

where

$$n_3 = \frac{n_2 + n_3}{g_2 + g_3} g_3, \quad n_2 = \frac{n_2 + n_3}{g_2 + g_3} g_2$$

is the total population of the Zeeman sublevels of states with  $F = 3$  and  $F = 2$  in the upper working level  $^2P_{1/2}$ ,  $g_3 = 7$  and  $g_2 = 5$  are their statistical weights (it is assumed that the population of the states is proportional to the static weights),  $n_1$  and  $g_1 = 24$  are, respectively, the population and statistical weight of the lower working level  $^2P_{3/2}$ , and  $|(m|\hat{\mu}|m')|^2$  are the squares of the moduli of matrix elements which determine the transition probabilities between the individual Zeeman sublevels and the intensity at the center of the line

$$\varphi(\omega) = \frac{\Delta\omega}{(\omega - \omega_0)^2 + (\Delta\omega)^2/4}$$

for each Zeeman component.

It is clear from the above expressions that the amplification coefficients differ from one another only by the values after the summation sign. Therefore, the construction of the resultant gain curves for the corre-

sponding groups of Zeeman components and their comparison can be carried out in relative units, without the use of the true level populations. The line width of an individual Zeeman component, which is necessary for the determination of the resultant profile, was taken from the paper by Zuev et al.,<sup>[9]</sup> but this resulted in an appreciable discrepancy between theory and experiment. In subsequent calculations we therefore used the line width obtained from our own data, using the observed equality of the amplification coefficients for the groups of  $\sigma$  components of the hyperfine transitions  $F = 3 - F = 4$  and  $F = 2 - F = 2$  at the time of switching, and the dependence of this time, i.e., the switching field on the gas pressure or, in the final analysis, on the width of the individual Zeeman component.

These calculations have shown that the amplification coefficients for the above groups of  $\sigma$  components can be equal only for a certain definite width of the Zeeman component. Thus, for a pressure of 22.5 Torr the line width of the emitted radiation was found to be  $0.015 \pm 0.0012 \text{ cm}^{-1}$ . This figure is obtained by combining two profiles, namely, a Lorentz and a Doppler profile. The Doppler broadening  $\Delta\nu_D = 0.011 \pm 0.001 \text{ cm}^{-1}$  was taken from our previous measurements<sup>[9]</sup> and corresponds to a medium temperature of  $530 \pm 100^\circ\text{K}$ . Collisional broadening was chosen so that the resultant profile ensured that the amplification coefficients for the corresponding groups of Zeeman components were equal for the required value of the magnetic field. It was found that  $\Delta\nu_L = 0.007 \pm 0.0005 \text{ cm}^{-1}$  which is lower by a factor of about two than the result reported in<sup>[9]</sup>.

Similarly, one can determine the emission line width of an individual Zeeman component when the gas pressure is increased by adding inert gases. Thus, at such pressures (200–300 Torr), the profile is of the purely Lorentz shape. It is then unnecessary to carry out the above combination of profiles and the problem is much simpler. For gas pressures of 247.5 Torr (22.5 Torr  $\text{C}_3\text{F}_7\text{I}$  and 225 Torr Ar), the line width was found to be  $0.07 \pm 0.005 \text{ cm}^{-1}$ , which meant that the broadening due to collisions with the argon gas exceeded by a factor of 1.5 the value obtained in<sup>[9]</sup>. If xenon is used as the added gas (total pressure 172.5 Torr, working gas pressure 22.5 Torr), the line width is found to be  $0.60 \pm 0.005 \text{ cm}^{-1}$ . The resultant gain curves obtained on the basis of the above line widths are in good agreement with experiment and can be used to explain many of the properties of the spectrum of stimulated radiation in the presence of a magnetic field. Thus, the measured frequencies shown in Fig. 3 (transverse field) and Fig. 4 (longitudinal field) are in good agreement with amplification maxima on the corresponding resultant curves shown by the solid lines for those values of the magnetic field for which these frequencies are present in the laser beam. Broken lines show the situation when they are not present in the stimulated emission under our conditions. Deviations which cannot be seen because of the frequency scale of Figs. 3 and 4 lie within the limits of experimental error.

Comparison of the amplification maxima on different resultant profiles, shown for the strongest groups of Zeeman components in Fig. 6 (transverse field) and Fig. 7 (longitudinal field), establishes a close correlation between their behavior in varying magnetic field and the spectral composition of the laser radiation. Thus, in complete agreement with experiment in the case of low

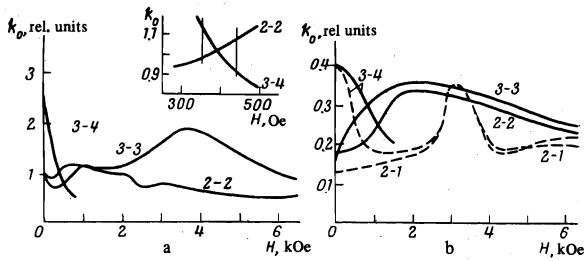


FIG. 6. Amplification coefficients for the strongest groups of Zeeman components in a transverse magnetic field; solid lines— $\sigma$  components; broken lines— $\pi$  components (values of  $F$  and  $F'$  are shown throughout, except for the insert, 2-2 and 3-3 should be interchanged).

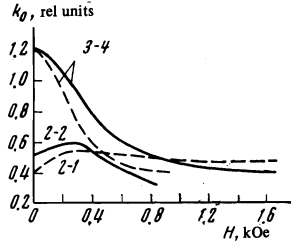


FIG. 7. Amplification coefficients for the strongest groups of Zeeman components in the longitudinal magnetic field: solid lines  $\pi^+$  components; broken lines  $\pi^-$  components (values of  $F$  and  $F'$  are indicated).

magnetic fields, the gain for the group of  $\sigma$  components of the  $F = 3 - F = 4$  transition is much greater than the gain for the other spectral components. However, this quantity very rapidly decreases because, as the field increases, the corresponding Zeeman components of the  $F = 3 - F = 4$  transition separate to distances comparable with the line width, and the contribution of each Zeeman component to the gain at the central frequency of the resultant profile falls much more rapidly than for the group of  $\sigma$  components of the 2-2 or 3-3 transitions (see [5]). Moreover, since the fields which we are considering are intermediate, an increase in the field is accompanied by a continuous change in the intensities of the Zeeman components: for the group of  $\sigma$  components of the 3-4 transition they rapidly fall, while for the group of the  $\sigma$  components of the 2-2 and 3-3 transitions they gradually increase. [5] As a result, the gain for the group of  $\sigma$  components of the 2-2 transition and then for the 3-3 transition, too, becomes higher than for the corresponding group of  $\sigma$  components of the 3-4 transition. We have thus reproduced all the changes in the spectral composition of the stimulated radiation which occurred when the magnetic field was increased. It is clear that analogous changes in the spectral composition are observed in the photodissociative laser when the uncompensated magnetic field due to the pumping source varies substantially during the generated pulse.

The ratio of the values of the amplification coefficients for which simultaneous generation of different groups of Zeeman components is still possible does not exceed 1.2 under our conditions with  $T_b = 10^4$  K. It is clear that this ratio is determined by the ratio of the rate of relaxation between sublevels of the upper state  $^2P_{1/2}$  with different  $F$ , and the probability of stimulated emission which is determined by the output power of the laser which, in turn, is very dependent on the pumping level. If we know the pumping energy, the output power, the generation threshold, and the ratio of the amplification coefficients for which simultaneous generation of the different components is still possible, we can try to estimate the relaxation which occurs between the two upper sublevels.

Under the above assumption of rapid collisional relaxation over the Zeeman sublevels of states with definite  $F$ , the kinetic equations for the atomic populations under our conditions can be written in the same form as for a laser in zero magnetic field [6]

$$\begin{aligned} \dot{N}_{31} &= f - k \frac{g_1}{g_3} N_1 (N_{31} - N_{21}) - c\sigma_{31} \left(1 + \frac{g_2}{g_1}\right) N_{31} n_{31}^{\text{ph}} - c\sigma_{21} \frac{g_2}{g_1} N_{21} n_{21}^{\text{ph}}, \\ \dot{N}_{21} &= f + k \frac{g_1}{g_3} N_1 (N_{31} - N_{21}) - c\sigma_{31} \frac{g_2}{g_1} N_{31} n_{31}^{\text{ph}} + c\sigma_{21} \left(1 + \frac{g_2}{g_1}\right) N_{21} n_{21}^{\text{ph}}, \\ \dot{N}_1 &= c\sigma_{31} \frac{g_2}{g_1} N_{31} n_{31}^{\text{ph}} + c\sigma_{21} \frac{g_2}{g_1} N_{21} n_{21}^{\text{ph}}, \\ n_{31}^{\text{ph}} &= -R n_{31}^{\text{ph}} + g_3 c\sigma_{31} N_{31} n_{31}^{\text{ph}}, \quad n_{21}^{\text{ph}} = -R n_{21}^{\text{ph}} + g_2 c\sigma_{21} N_{21} n_{21}^{\text{ph}}, \end{aligned} \quad (2)$$

where

$$N_{31} = n_3 / g_3 - n_1 / g_1, \quad N_{21} = n_2 / g_2 - n_1 / g_1, \quad N_1 = n_1 / g_1,$$

$n_{31}^{\text{ph}}$  and  $n_{21}^{\text{ph}}$  are the densities of photons with corresponding frequencies,  $k = \langle \sigma \nu \rangle (g_2 + g_3) / g_2 g_3$  is a constant which governs the rate of transition between the excited states with  $F = 3$  and  $F = 2$  during collisions with unexcited iodine atoms,  $1/R$  is the lifetime of a photon in the resonator,

$$N_{31}^{\text{th}} = R / g_3 c\sigma_{31}, \quad N_{21}^{\text{th}} = R / g_2 c\sigma_{21},$$

and  $\sigma_{31}$  and  $\sigma_{32}$  are the corresponding gain cross sections calculated for the required fields. The pump pulse is assumed to have the triangular form

$$f(t) = at, \quad 0 \leq t \leq \tau_0, \\ f(t) = 2a\tau_0 - at, \quad \tau_0 \leq t \leq 2\tau_0,$$

where  $t = \tau_0$  corresponds to the pulse maximum.

If  $\sigma_{31} > \sigma_{21}$ , then  $N_{31}^{\text{th}} < N_{21}^{\text{th}}$  and generation begins on the 3-1 transition. Assuming that for a strong transition we can set  $N_{31} = 0$ ,  $N_{31}(t) = N_{31}^{\text{th}}$ , we obtain the equation for  $N_{21}(t)$  which we shall solve subject to the initial condition  $N_{21}(t_0) = N_{31}^{\text{th}}$ . Here,  $t_0 = (2N_{31}^{\text{th}}/\alpha)^{1/2}$  is the beginning of generation from the strong transition. The resulting equation for  $N_{21}(t)/N_{31}^{\text{th}} = \varphi(t)$  can be written in the form

$$\begin{aligned} \dot{\varphi} &= 0.77 \frac{f(t)}{N_{31}^{\text{th}}} + D \left[ \varphi^2 + 0.4\varphi - 1.4 - (\varphi - 1) \frac{2.4}{N_{31}^{\text{th}}} \int_0^t f(t') dt' \right], \\ \varphi(t_0) &= 1. \quad D = \frac{g_1}{g_1 + g_3} \langle \sigma \nu \rangle N_{31}^{\text{th}} \frac{g_2 + g_3}{g_2 g_3}. \end{aligned} \quad (3)$$

Computer solutions of Eq. (3) for different values of  $D$  are shown in Fig. 8.

Using the fact that the ratio  $N_{21}(t)/N_{31}^{\text{th}}$ , for which the weak component appears in the generated radiation, is equal to 1.2, we find the corresponding value of  $D$ . Taking as the criterion the increase above 1.2 for a certain minimum time (a few microseconds, see Fig. 5d), we find that  $D \approx 1.7 \times 10^5$ . Hence, we find that  $\langle \sigma \nu \rangle \approx 1.08 \times 10^{-9} \text{ cm}^3/\text{sec}$ , which differs somewhat from the theoretical estimate  $\langle \sigma \nu \rangle = 1.5 \times 10^{-9} \text{ cm}^3/\text{sec}$  given in [6].

Using the calculated value of  $k$ , we find that  $\varphi_{\text{max}}$  in zero magnetic field with  $T_b = 10^4$  K amounts to 1.46, i.e., the generation threshold for the 2-2 component is not reached. Therefore, under these conditions this component could not be observed. As the pump energy is increased, higher values of  $\varphi$  exceeding even 2.3 are achieved. As a result, the 2-2 component may appear even for zero magnetic field and this did, in fact, occur in our experiment with  $T_b = 13\,000$  K for which we

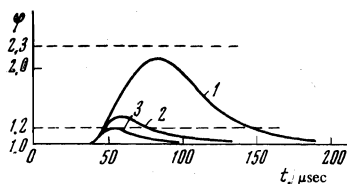


FIG. 8. Plot of the function  $\phi = N_{2i}(t)/N_{31i}^{th}$ .

observed weak traces of this component because the pumping energy was still insufficient. By using higher pumping levels it is probably possible to establish conditions for stable generation of the weak component in zero magnetic field, observed in<sup>[6]</sup>. A substantial increase in the pumping level is accompanied by a change in the spectral composition of the laser radiation when the magnetic field is present. However, these changes occur in complete accordance with the amplification coefficients given in Figs. 6 and 7 for the different groups of components.

The above theoretical analysis does not explain some of the observed features of the weak component as a function of time (Figs. 5a, b, c, d), i.e., its multiple appearance during the laser pulse. This is probably connected with the fact that when the equations were solved, we did not take into account the relaxation of the ground state of the iodine atom, which is not negligible.<sup>[10,11]</sup>

## CONCLUSION

We have investigated the behavior of the spectrum of stimulated radiation in different magnetic fields, including zero field, and have determined experimentally the hyperfine structure constant for the upper working level of the iodine atom,  $A_{1/2}$ . We have also found the line broadening for the working transition of the iodine atom during collisions with  $C_3F_7I$  molecules and the atoms of argon and xenon, which can be used to determine the corresponding broadening cross sections and the van der Waals constants for the interactions between the iodine atom and the gases. The calculated frequencies and amplification coefficients for the strongest groups of Zeeman components have enabled us to explain the behavior of the spectrum of stimulated radiation in a varying magnetic field. We have estimated the relaxation between sublevels of the upper working state  $^2P_{1/2}$  with different  $F$ .

The above study of the spectral composition of stim-

ulated radiation due to the  $^2P_{1/2} - ^2P_{3/2}$  transition in the iodine atom has shown that the radiation kinetics of the above laser, which is a complicated spectral system, depends on many factors such as the magnetic field, working gas pressure, and pumping energy. The characteristics of the laser beam are determined not only by the chemical reaction kinetics but also by the structure of the upper and lower states involved in the transition, and vary even during the laser pulse. This must be taken into account when different kinetic models are set up for the iodine photodissociative laser. More detailed analyses of the laser spectrum in a magnetic field will have to take into account the kinetics of populations of all the sublevels involved in the particular transition.

The authors are greatly indebted to N. N. Rozanov for useful discussions.

- <sup>1</sup>I. M. Belousova, V. M. Kiselev, and V. N. Kurzenkov, *Opt. Spektrosk.* **33**, 203 (1972).
- <sup>2</sup>W. C. Hwang and J. V. V. Kasper, *Chem. Phys. Lett.* **13**, 511 (1972).
- <sup>3</sup>M. I. D'yakonov and S. A. Fridrikhov, *Usp. Fiz. Nauk* **90**, 565 (1966) [*Sov. Phys.-Usp.* **9**, 837 (1967)].
- <sup>4</sup>I. M. Belousova, V. M. Kiselev, and V. N. Kurzenkov, *Opt. Spektrosk.* **33**, 210 (1972).
- <sup>5</sup>I. M. Belousova, B. D. Bobrov, V. M. Kiselev, V. N. Kurzenkov, and P. I. Krepostnov, *Opt. Spektrosk.* **36**, 6 (1973).
- <sup>6</sup>V. A. Alekseev, T. L. Andreeva, V. N. Volkov, and E. A. Yujov, *Zh. Eksp. Teor. Fiz.* **63**, 452 (1972) [*Sov. Phys.-JETP* **36**, 238 (1973)].
- <sup>7</sup>V. Jacarino, J. G. King, R. A. Satten, and H. Stroke, *Phys. Rev.* **94**, 1798 (1954).
- <sup>8</sup>V. Yu. Zelesskiĭ, Yu. M. Ivanenko, and T. I. Krupenikova, *Opt. Spektrosk.* **35**, 6 (1973).
- <sup>9</sup>V. S. Zuev, V. A. Katulin, V. Yu. Nosach, and O. Yu. Nosach, *Zh. Eksp. Teor. Fiz.* **62**, 1673 (1972) [*Sov. Phys.-JETP* **35**, 870 (1972)].
- <sup>10</sup>T. L. Andreeva, S. V. Kuznetsova, A. I. Maslov, I. I. Sobel'man, and V. N. Sorokin, *ZhETF Pis. Red.* **13**, 631 (1971) [*JETP* **13**, 449 (1971)].
- <sup>11</sup>I. M. Belousova, N. G. Gorshkov, O. B. Danilov, V. Yu. Zalesskiĭ, and I. L. Yachnev, *Zh. Eksp. Teor. Fiz.* **65**, 517 (1973) [*Sov. Phys.-JETP* **38**, 254(1974)].

Translated by S. Chomet

55